IEEE Photonics Journal
An IEEE Photonics Society Publication

Open Access

Path-Loss Optimized Indoor Laser-Based Visible Light Communication System for Variable Link Length Gigabit-Class Communication

Volume 12, Number 4, August 2020

Faheem Ahmad, *Member, IEEE*
Sathisha Ramachandrapura, *Member, IEEE*
Jyothsna Konkada Manattayil, *Member, IEEE*
Varun Raghunathan, *Senior Member, IEEE*

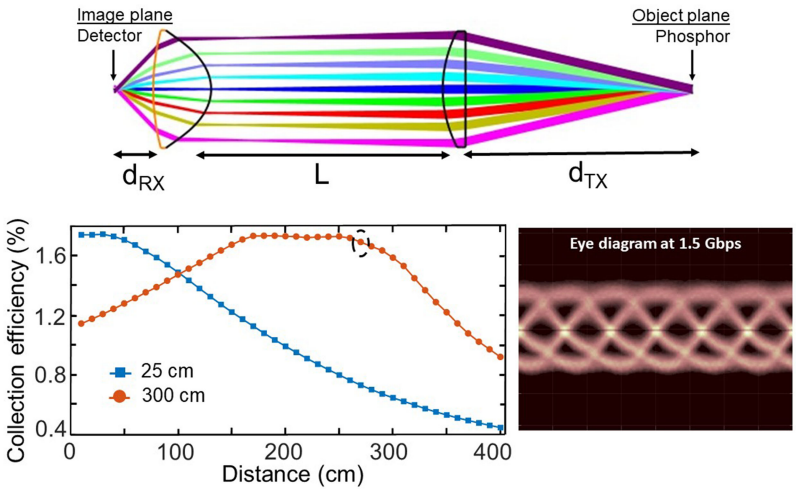

DOI: 10.1109/JPHOT.2020.3014216

Path-Loss Optimized Indoor Laser-Based Visible Light Communication System for Variable Link Length Gigabit-Class Communication

**Faheem Ahmad, *Member, IEEE*,
Sathisha Ramachandrapura, *Member, IEEE*,
Jyothsna Konkada Manattayil, *Member, IEEE*,
and Varun Raghunathan, *Senior Member, IEEE***

Electrical Communication Engineering Department, Indian Institute of Science, Bangalore 560012, India

DOI:10.1109/JPHOT.2020.3014216

Manuscript received April 28, 2020; revised July 21, 2020; accepted July 30, 2020. Date of publication August 4, 2020; date of current version August 13, 2020. This work was supported by Department of Telecommunication, Government of India through the Indigenous 5G Testbed project. Corresponding author: Varun Raghunathan. (e-mail: varunr@iisc.ac.in).

Abstract: We discuss an optical ray-tracing approach for minimizing path-loss in a variable link length indoor blue laser down-converted white light visible light communication (VLC) system. For a given link length, minimum path-loss is achieved by finding optimum positions of transmitter and receiver lenses relative to phosphor and detector respectively such that collection efficiency is maximized. The designed VLC system is experimentally implemented for two different optimized link lengths of 25 and 300 cm. The down-converted white light for the optimized link is found to exhibit narrow beam spread, spot-lighting type illumination profile. The white light is measured to quantify the beam profile, color rendering, illuminance and percentage of blue-content. The illumination beam profile and propagation characteristics are found to be in good agreement with optical simulations. Communication experiments with on-off modulation at 1.5 Gbps achieved BER of $\sim 3 \times 10^{-3}$ for the optimized link, which is below the forward-error correction threshold. The above communication performance is achieved at illumination levels at the receiver as low as $\sim$45 and 16 lx. Comparison with previous laser-based VLC implementations shows that the path-loss optimization helps achieve gigabit-class communication at practically relevant link lengths and the lowest illuminance levels thus far reported. Such low illuminance level, narrow beam spread VLC luminaires can potentially coexist with existing lighting infrastructure for eye-safe indoor applications.

Index Terms: Free-space communication, Advanced optics design, Visible lasers, Photodetectors, Solid-state lighting.

1. Introduction

Visible light communication (VLC) offers a promising solution to meet the need for high data-rate communication in indoor settings by leveraging solid-state lighting installations for short range free-space optical communication [1], [2]. This is motivated by the large, un-licensed bandwidth available in the optical spectrum, the inherent small-cell architecture of illumination light sources and the absence of RF interference with the use of optical waves [2]. For such implementations

to be of practical relevance, the transmitter-to-receiver separation distance required are typically in the range of 1–5 meters, depending on the specific use-case, with indoor illuminance levels in the range of 300–500 lx. Light emitting diodes (LEDs) have been successfully utilized for implementing VLC with data rates exceeding few Gigabit-per second (Gbps) [3]–[6]. However, the inherent low modulation bandwidth of LEDs increases the complexity of the electronic hardware required to implement high data-rate communication utilizing advanced modulation formats. This bandwidth limitation with LEDs is overcome to some extent with the use of emerging micro- and resonant-LED based transmitters [7], [8]. Another promising direction is the utility of laser diodes (LD) for indoor VLC application [9]–[13]. LDs offer much wider modulation bandwidth when compared to LEDs and hence are better suited for data communication [14]. Data modulated blue LDs incident on remote phosphors are used to down-convert the narrow blue laser spectrum to broadband white light for illumination purpose [15]. At the receiver end, the remnant blue light is detected for data communication. The use of phosphors with diffusive surfaces result in the remnant blue light experiencing larger angular spread with reduced spatial coherence when compared to the highly coherent laser diode. The reduced spatial coherence of the blue light and its down-conversion to incoherent white light can help in ensuring eye-safety of such laser-based VLC transmitters when used in indoor settings [16]. With laser-based VLC links, data-rate as high as 2 Gbps using simple on-off keying modulation has been demonstrated for link length of 5 cm [9]. The data throughputs have been further improved using OFDM techniques, for example 6.52 Gbps data-rate at 1000 lx light level has been demonstrated for link length of 15 cm [10]. Red, green and blue (RGB) LDs have also been combined at appropriate power level and incident on a diffusive surface for white light generation through color mixing [12], [13]. Aggregated data rate as high as 14 Gbps has been demonstrated with such RGB LDs using 16-QAM OFDM for a link range of 30 cm [12].

Most of the previous LED- and LD-based indoor VLC demonstrations have achieved the best communication performance at link lengths typically limited to tens of centimeters to at best a meter. This is mainly due to signal to noise ratio deterioration at longer lengths. An increase in the illuminance level is often suggested as a solution to increase link distance. This however results in additional power penalty and possible eye safety issues. In one such longer range VLC implementation with multicolor LED transmitters, an aggregated data-rate of $\sim$5 Gbps was achieved with illuminance level increased to 720 lx in order to support link lengths of 400 cm [17]. There are also reports of low-power directed laser beams to extend the range to tens of meter for indoor VLC [18]. However, the high spatial coherence of directed laser beams is still a concern for eye-safety in indoor setting, as the laser can be focused onto the retina even at low power levels resulting in high optical intensity levels [16]. Thus, it is desirable to achieve the best communication performance at practically relevant link lengths without incurring any additional power penalty or compromising on eye-safety.

In this context, we present an optical ray-tracing based approach for minimizing path-loss and hence increase light throughput in a variable link length LD-based indoor VLC system. Optical ray-tracing has been utilized previously to find appropriate lenses for the design of imaging-based VLC link [8]. However, the role of ray-tracing in optimizing optical throughput of a VLC link has not been studied before in any detail. The optical throughput of the VLC link is best characterized by path-loss or inverse of collection efficiency at the receiver [2]. The path-loss accounts for the fact that not all the light directed from transmitter is collected at the receiver due to beam divergence or obstructions in the optical path. The path loss optimization procedure described here is aimed at finding optimum positions of transmitter and receiver lenses relative to the remote phosphor and detector respectively in a directed line-of-sight link such that the collection efficiency is maximized. The optimization methodology presented here provides a useful tool to achieve maximum throughput for different link distances with minimal modification to the VLC link by just varying transmitter and receiver lens positions. The VLC link is experimentally implemented here for two different optimizations at link lengths of 25 and 300 cm. Communication experiments with on-off modulation at maximum data-rate of 1.5 Gbps achieves bit-error rate of $\sim 3 \times 10^{-3}$, which is below the threshold for implementing forward-error correction. The best communication

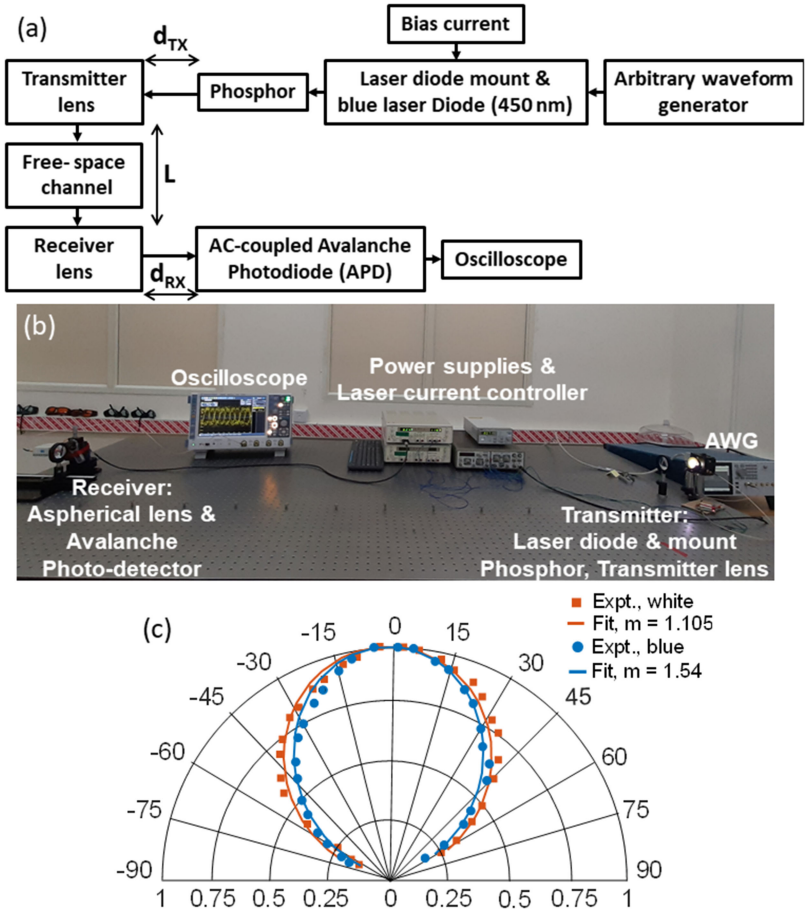

Fig. 1. (a) Schematic block diagram of the VLC set-up studied in this work. (b) Photograph of the experimental set-up implemented with the components labelled. (c) Experimentally measured angular divergence profile and fit for the blue light and down-converted white light after the phosphor.

performance is achieved at illuminance levels as low as 45 and 16 lx respectively with narrow beam spread, spot-light type illumination profile. A comparison with previous LD-based indoor VLC implementations shows that our path-loss optimization procedure helps achieve high fidelity, gigabit class communication at increased link lengths and lowest illuminance levels thus far reported. Such low illuminance level, narrow beam spread VLC luminaires can potentially coexist with lighting infrastructure for indoor applications. The work presented here also underscores the importance of optical system design, or in particular ray-tracing to maximize light throughput to achieve good communication and illumination performance at practically useful link lengths.

2. Description of Visible Light Communication System

A schematic block diagram of the LD-based VLC link considered in this work and a photograph of the implemented VLC set-up are shown in Fig. 1(a) and (b) respectively. An arbitrary waveform generator (Tektronix, AWG520) is used as the source of pseudo-random bit sequence (PRBS) for the communication experiments. This is subsequently amplified to 2 V peak-to-peak level and is combined with the laser bias using a bias-T integrated with the LD driver module (Thorlabs LDM9T). A blue LD with 450 nm center wavelength (Osram PL450B) is used as the light source. The modulation bandwidth of the LD is limited by the driver module to ~800 MHz. For nominal bias

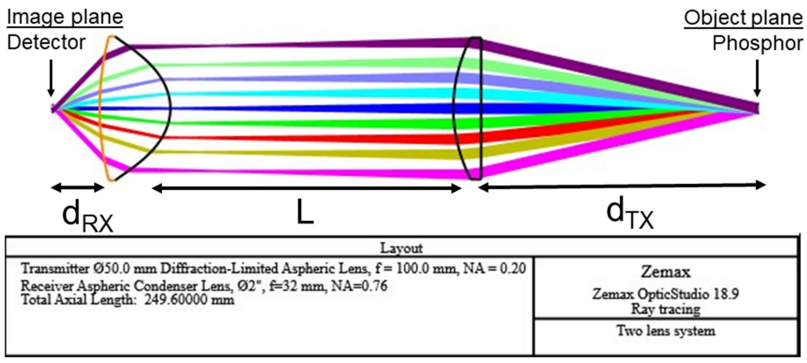

Fig. 2. Ray-tracing layout of the VLC link showing the phosphor surface (object plane) and detector (image plane) with separation of phosphor to transmitter lens as d_{TX} and receiver lens to detector as d_{RX}. The link distance between the transmitter and receiver lens is L.

current of 50 mA used for the VLC experiments, output optical power of 28 mW is obtained from the LD. The modulated laser with an elliptical spot of 2x6 mm diameter is incident on a warm-white remote phosphor (Intematix 2700K, CL-827-R75-PC [19]) to down-convert the incident blue light to broadband white light. The Lambertian profile of the emitted light from the phosphor surface is modeled as $\cos^m(\theta)$ function with a Lambertian parameter, m [20]. The measured beam profiles for the blue and down-converted white light after the phosphor surface are shown in Fig. 1(c). By fitting the measured data to a Lambertian profile, the Lambertian parameter is obtained as m $=$ 1.54 and 1.105, with the corresponding measured semi-angles of $\sim$50.4º and 57.7° for blue and white light respectively. The diffusive surface of the phosphor increases the angular spread of the blue light as measured above and results in reduced spatial coherence. The light emitted from the phosphor surface is loosely directed towards the receiver using a 5 cm diameter, 10 cm focal length single aspherical lens (AL50100M-A) with numerical aperture of 0.24. At the receiver side, a 5 cm diameter, 3.2 cm focal length single aspherical lens (ACL50832U-A) with numerical aperture of 0.76 is used to focus the received light onto the photodetector. An AC-coupled avalanche photodetector (Hamamatsu C5658) with 0.5 mm diameter sensor is used as the photodetector. The low frequency modulation background due to ambient lighting and the down-converted light is partially rejected using the AC-coupled detector. A band-pass blue filter (450 $+/-$20 nm) is also used before the detector to further reject the ambient and down-converted light which can potentially contribute to low-frequency noise [21]. The bandwidth of the photodetector is limited to $\sim$1 GHz. The detected waveforms are acquired in an oscilloscope (Rohde and Schwarz, 5000 series) and processed offline to obtain eye-diagrams.

3. Optical Ray-Tracing Studies

Ray tracing of the VLC optical link is implemented in Zemax optical design software in sequential mode [22]. The purpose of this study is to maximize collection efficiency or minimize path-loss across the optical link at the communication wavelength centered at 450 nm. The optical layout for a typical VLC link showing the transmitter and receiver, as captured from Zemax with the phosphor surface acting as the object plane and the detector surface as the image plane is shown in Fig. 2. For the ease of implementation, we use stock lenses at the transmitter and receiver side. The transmitter and receiver lenses of focal lengths 10 cm and 3.2 cm respectively are chosen to ensure effective demagnification of the illumination spot. This resembles an imaging-based VLC link [23], [24], [8], typically used in multiple-input multiple-output (MIMO) implementation with the objective of achieving wide-field imaging of multiple light sources onto multiple detectors. In the present paper, the main emphasize is placed on maximizing light throughput for a single-input

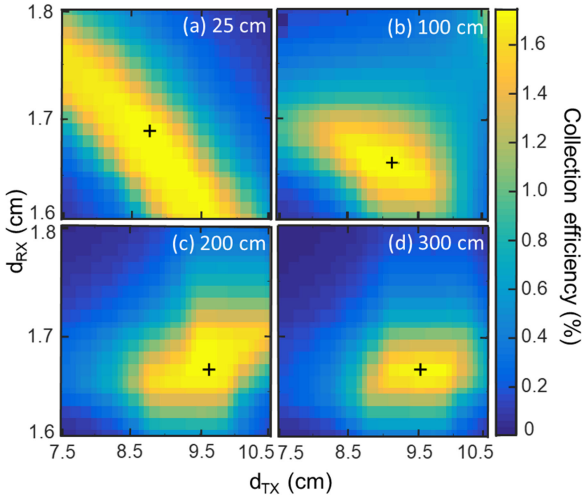

Fig. 3. Contour maps showing collection efficiency as a function of varying transmitter and receiver lens positions relative to the phosphor and detector respectively for link optimized for L = (a) 25 cm, (b) 100 cm, (c) 200 cm, and (d) 300 cm. The maximum collection efficiency point is marked by '+'. This corresponds to optimum d_{TX}, d_{RX} of: (a) 8.75, 1.69, (b) 9.14, 1.66, (c) 9.63, 1.67, and (d) 9.53, 1.67 respectively (all values are in units of cm).

single-output (SISO) implementation by utilizing detailed ray-tracing study. Furthermore, the ability to maximize collection efficiency at variable link distances with minimal changes to the VLC link is also studied.

The collection efficiency or inverse of path-loss is calculated as the fraction of the rays received at the detector plane appropriately weighed by the Lambertian source profile. The collection efficiency, η at the receiver is given by:

$$\eta = \frac{\int_0^{\theta_{max}} \rho(\theta) . \sin(\theta) . \cos^m(\theta) . d\theta}{\int_0^{\theta_{max}} \sin(\theta) . \cos^m(\theta) . d\theta} \quad (1)$$

where $\rho(\theta)$ refers to the fraction of the un-vignetted rays as a function of the object field-angle θ with the maximum angle, $\theta_{max} = 90^o$. $Cos^m(\theta)$ representing the Lambertian profile of the light emitted from the phosphor surface, as discussed above. For the ray tracing studies, the rays emitted from the phosphor plane within an angular range of 0 to 20° in steps of 0.01° are considered. This angular range includes all the rays within the collection angle of the transmitter lens for the range of working distances considered here. The distance between the phosphor and the transmitter lens (denoted as d_{TX}) and the distance between the receiver lens and phosphor (denoted as d_{RX}) are considered as variables for optimization with the objective of achieving maximum collection efficiency for a fixed transmitter-to-receiver separation distance (denoted as L).

Fig. 3 shows contour maps of collection efficiencies at the blue laser wavelength as a function of d_{TX} and d_{RX} for link distances of L = 25, 100, 200 and 300 cm. This represents use-case scenarios in which the VLC link can vary from short to long range in an indoor setting, for example from a desk lamp to ceiling light fixture used as the VLC transmitter. The optimum position of the lenses corresponding to the maximum collection efficiency, denoted by '+' in each of the contour plots. For small values of L, multiple combinations of d_{TX} and d_{RX} achieve close to the maximum collection efficiency with a decrease in d_{TX} from its back focal position compensated by an increase in d_{RX} or vice versa. With increasing L, the region of maximum collection efficiency is found to shrink in the contour map. This is a result of the lens positions nearing the respective back focal distances to ensure maximum light throughput for increased link lengths. Fig. 4(a) shows the path-loss curves depicting variation of collection efficiency verses link distance for d_{TX} and d_{RX} fixed at positions optimized for L = 25 cm and 300 cm. The path-loss curves reach a maximum value close to the

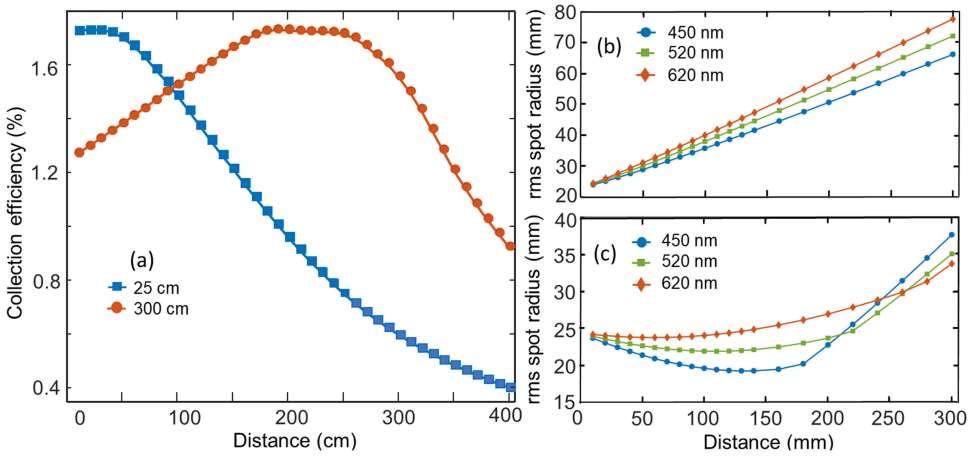

Fig. 4. (a) Variation of collection efficiency versus distance for link optimized for L = 25 cm (blue curve) and 300 cm (red curve). Variation of the rms spot radius of the ray scatter plot as a function of distance for link optimized for: (b) L = 25 cm and (c) L = 300 cm. (b), (c) are shown for three different wavelengths: 450 nm (blue curve), 520 nm (green curve), and 620 nm (red curve).

optimized link distance. It is however found that with increasing optimized distance, the path-loss curve reaches a plateau around 200-250 cm and decreases further. This is seen for the L = 300 cm path-loss curve in Fig. 4(a). This is again a consequence of the lens positions nearing the back focal distances for longer link lengths, which results in collection efficiency maximized at an intermediate plane. Collection efficiencies of 1.72% and 1.58% are obtained for L = 25 cm and L = 300 cm optimized links respectively. We have also investigated the sensitivity of the path-loss optimized link for receiver offset from the optical axis to model non-directed line-of-sight communication. It is found that the maximum collection efficiency drops by 50% for receiver placed at $+/-1.74$ cm and $+/-2.54$ cm for receiver placed at optimized positions of L = 25 cm and 300 cm respectively. This shows that the receiver can tolerate few centimeters of offset from the optical axis and still achieve good light throughput for data communication.

The best collection efficiency achievable for light emitted from an extended source is limited by the overall optical throughput of the system. It is thus useful to compare the above collection efficiency with the ideal throughput of the optical link calculated as the ratio of étendue between the detector and the phosphor planes, when placed at the back focal distance. Isotropic emission and collection profiles are assumed for this calculation. The étendue at the detector and phosphor planes, calculated as the product of the area of the optical beam and the solid angle subtended is found to be 0.432 mm^2-Sr and 21.158 mm^2-Sr respectively, resulting in an expected throughput of 2.04%. Thus, the collection efficiency obtained by optical ray-tracing is found to be close to the ideal throughput expected for the present VLC optical link using single transmitter and receiver lenses.

The path-loss optimization described above is performed at the blue laser diode wavelength of 450 nm. The illumination beam quality is evaluated here using root-mean square (rms) spot radius obtained from the ray-scatter plots for blue (450 nm), green (520 nm) and red (620 nm) wavelengths. Fig. 4 (b) and (c) shows the rms spot radii for the path-loss optimized link at L = 25 cm and 300 cm respectively. It is found that the VLC link optimized at the communication wavelength results in the blue, green and red components propagating with slightly different spatial characteristics. For the link optimized at L = 25 cm, the illumination spot is found to diverge as it propagates towards the receiver with a maximum spot radius of 2.7 cm at the optimized distance. For the link optimized for L = 300 cm, the illumination spots are found to nominally focus at an intermediate plane before reaching the receiver plane with a spot radius of 3.8 cm at the optimized distance. The observed propagation characteristics above are a result of d_{TX} less than

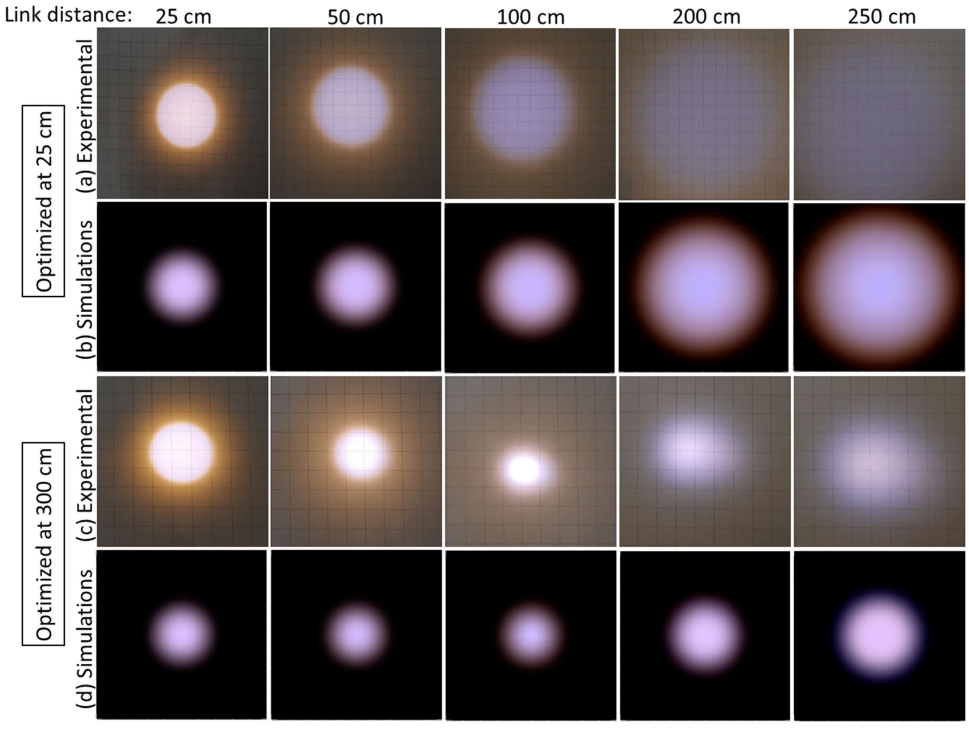

Fig. 5. Comparison of the experimentally measured illumination spot (a, c) and the simulated circular aperture images (b, d) for the VLC link optimized for: (a, b) 25 cm and (c, d) 300 cm. The grid chart for the experimental images has a spacing of 1.25 cm and the simulated image size is 11.5 $\times$ 11.5 cm.

and comparable to the back-focal length of the transmitter lens respectively for the two optimized conditions. The overall deviation in the rms spot radius is found to be below 7% for the three wavelengths considered at the optimized receiver plane. In comparison with conventional light sources used for indoor illumination application, the path-loss optimized light source experiences narrow beam spread as it propagates towards the receiver. The optimized VLC luminaire resembles a spot-light type illumination profile with spot diameter less than 10 cm at the optimized receiver plane. For the present optical design, with the transmitter and receiver lenses placed at their respective back focal distances, the maximum angular field-of-view is estimated to be 1.7^{o} and 0.45^{o} respectively.

4. Experimental Results

In this section, experimental characterization of the VLC link to measure the white light illumination quality and data communication performance are discussed. These measurements are performed with the VLC link optimized for L = 25 and 300 cm by precisely measuring the distance between the transmitter (receiver) lens and phosphor (photodetector) to within 0.5 mm accuracy. The maximum link length used in the experimental measurements is however limited to 265 cm by the length of the optical table used in this implementation. Nonetheless, the L = 300 cm optimization results in maximum collection efficiency at 265 cm as well, as seen from Fig. 4(a).

Fig. 5 shows the comparison of the experimental and simulated illumination spots for the two optimized VLC links as a function of varying distance along the optical path. The experimental illumination spots are obtained by taking photographs along the VLC link using a grid chart with grid lines spaced 1.25 cm apart. The simulated illumination spots are obtained using image simulation of a circular aperture in Zemax in non-sequential mode [22]. The color content of the

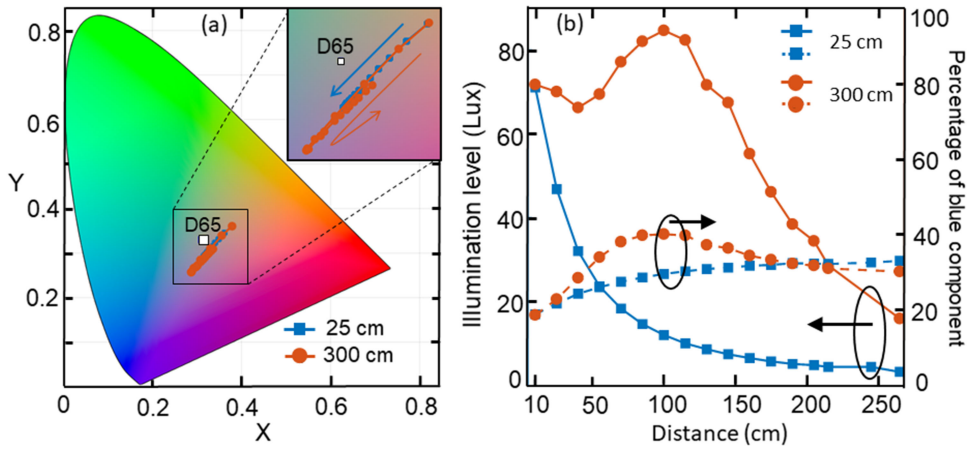

Fig. 6. (a) Color co-ordinates of the white light generated in the VLC link plotted in the color gamut map for L = 25 cm (blue points) and L = 300 cm (red points) optimized link. The inset shows a zoomed in view with the arrow indicating the variation with increasing link distance. (b) Variation of the illuminance level (in lux) – left axis with solid curves and the measured percentage of blue content – right axis with dashed curves as a function increasing link distance for the VLC link optimized for L = 25 cm (blue curves) and L = 300 cm (red curves).

white illumination spot in the experimental and simulated results are not identical, as observed by the yellowish warm white color observed in the experimental images and cooler-white color in the simulated plots. Nonetheless, very good qualitative agreement between the propagation of the illumination spot in the experimental and simulated images is obtained. This is observed by the continuous divergence of the spot for L = 25 cm optimized link and the initial focusing followed by divergence for L = 300 cm optimized link. This is consistent with the ray-tracing results shown in Fig. 4(b) and (c). Furthermore, similar propagation characteristics for the various wavelength components of white light are observed in both experimental and simulated images. This is evident from the slight blueish central spot with yellow halo observed for L = 25 cm optimized link and the opposite profile for L = 300 cm optimized link. The measured beam radii of the illumination profile are ~3.1 cm and 4.4 cm at 25 cm and 250 cm, obtained from Fig. 5(a) and (c) respectively, which are found to be comparable to the simulated rms spot radius discussed in Section 3 above.

Next, the white light characteristics measured using Sekonic C-800 spectrometer are discussed. The diffusive surface of the spectrometer placed normal to the illumination spot at its center is used to measure the spectrum, illuminance level, color co-ordinates and color temperature. Fig. 6(a) shows the color co-ordinates plotted in the CIE 1931 XY color space. The comparison of the measured color co-ordinates with standard D65 white light is also shown. With increasing distance, the color point shifts diagonally downwards towards more bluish colors. The illumination source in the VLC system exhibits chromaticity shifts as a function of distance from light source to the intended illumination plane. The impact of such shifts on the illumination performance in a VLC link has not been quantified in previous reports. For L = 300 cm optimization (shown by the orange curve) the color point is found to shift towards bluish illumination and retrace back towards the D65 point. At the intended illumination plane for the two optimized VLC links (25 cm and 265 cm), the measured (X, Y) color co-ordinates are (0.362, 0.345) and (0.326, 0.309) respectively, with correlated color temperatures (CCT) of 4344 and 5265 respectively and color rendering indices (CRI) of 86.9 and 89.1 respectively. Fig. 6(b) shows the illuminance levels (solid curves – left axis) and percentage of blue content (dashed curves – right axis) as a function of distance along the VLC link. For L = 25 cm optimized link, the illuminance level is found to decrease monotonically with the blue color content slightly increasing and saturating. In contrast, for L = 300 cm optimized link, the illuminance level and blue content are found to peak at

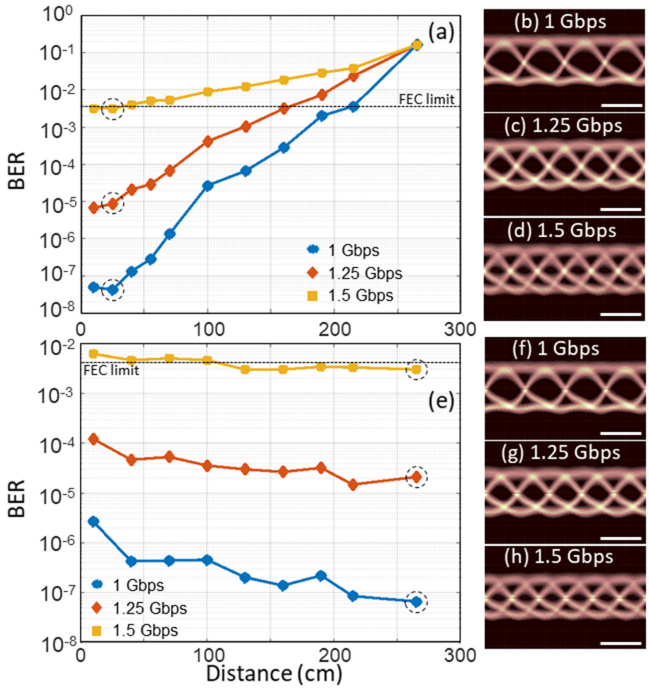

Fig. 7. (a) BER versus VLC link length for the optical system optimized for L = 25 cm. Representative eye-diagrams used to extract the BER for data-rate of: (b) 1Gbps, (c) 1.25 Gbps, and (d) 1.5 Gbps. The BER points corresponding to the shown eye-diagrams are denoted by dashed circles in (a). (e) BER versus VLC link length for the optical system optimized for L = 300 cm. Representative eye-diagrams used to extract the BER for data-rate of: (f) 1Gbps, (g) 1.25 Gbps, and (h) 1.5 Gbps scale bar for the eye diagrams corresponds to 1 nsec. The BER points corresponding to the shown eye-diagrams are denoted by dashed circles in (e). Forward error-correction (FEC) limit is shown by the horizontal dashed line in (a) and (e).

distance of ∼100 cm and subsequently decrease due to the initial focusing followed by divergence of the illumination spot along the free-space link. For the two link optimizations, the measured illuminance level are 45 lx and 16 lx at 25 cm and 265 cm link distance respectively, resulting in blue light intensity levels of 37 μW/cm^2 and 12 μW/cm^2 respectively. The optical ray-tracing studies combined with the illumination characterization discussed here can be used to guide the design of optical transmitters in a VLC system.

Next, the communication performance of the VLC link is characterized by directly modulating the blue laser diode with on-off keying (OOK), pseudo-random bit sequence (PRBS) waveform with $2^{15} - 1$ bits generated using the arbitrary waveform generator. At the receiver end, the detected electrical waveforms acquired using the oscilloscope is processed offline using MATLAB eye-diagram toolbox to obtain bit-error rate (BER). Fig. 7(a) and (e) shows the variation of the BER measured along the link length for the two link optimizations. Each of these plots shows the BER for OOK data transmission at data-rates of 1 Gbps, 1.25 Gbps and 1.5 Gbps. Representative eye-diagrams used to calculate the BER are also shown in Fig. 7 for the BER points shown by the circles. The BER obtained at 25 cm, as shown in Fig. 7(a) are 4×10^{-8}, 9×10^{-6}, and 3.3×10^{-3} respectively, while the BER obtained at 265 cm, as shown in Fig. 7(e) are 7×10^{-8}, 2×10^{-5}, and 3×10^{-3} respectively for the three data rates considered. The BERs obtained are below the forward-error correction (FEC) limit of 3.8×10^{-3} for practical communication system implementation. The observed variation of BER with link distance as shown in Fig. 7 is attributed to the variation in collection efficiency due to path-loss optimization, resulting in better signal to noise ratio and hence lower BER for the received waveforms when measured close to the optimized receiver plane.

TABLE 1
A Comparison of Present Work With Previous Implementations of LD-Based VLC With OOK Modulation

Implementation [Ref]	Link length (cm)	Laser power (mW)	Illuminance / Luminous flux	CCT (K)	Data rate (Gbps)	BER
450 nm LD phosphor down-converted white light [9]	5	375	50 lm	4740	2	3.5×10^{-3}
410 nm LD, RGB phosphor down-converted white light [25]	15	70	-	4050	1.5	1.8×10^{-3}
450 nm LD phosphor down-converted white light [26]	100 150	-	750 lx 550 lx	5000	1.25 1.05	4.5×10^{-5} 1×10^{-4}
Directed 450nm LD (no phosphor) [27]	15	130	-	-	4	2.7×10^{-4}
Directed 680nm LD (no phosphor) [18]	1200	0.6	150 lx	-	2.5	9×10^{-4}
This work: Path-loss optimized 450 nm LD phosphor down-converted white light	265	28	16 lx	5265	1 1.25 1.5	7×10^{-8} 2×10^{-5} 3×10^{-3}

5. Discussion

We compare the performance of the present LD-based VLC implementation with previous demonstrations utilizing OOK modulation in Table 1. We restrict this comparison to OOK modulation only in order to directly compare the link distance, data rates and BER across different implementations. It is well known that further improvement in communication performance can be achieved with the use of advanced modulation formats such as discrete multi-tone (DMT) or orthogonal frequency division multiplexing (OFDM) techniques [4], [7]. As seen from Table 1, the present work achieves gigabit-class communication performance with white light illumination source for maximum link length of 265 cm and illumination level as low as 16 lx. In the context of LD-based white light VLC systems, the present demonstration represents the longest link length combined with lowest illuminance level at the receiver, however at slightly higher CCT levels. The data-rates can be improved further in the present implementation keeping the illuminance levels fixed by increasing the modulation bandwidth of laser driver, incorporating suitable equalization techniques and by the implementation of advanced modulation formats as discussed above.

The white light illumination profile obtained in the path-loss optimized link as shown in Fig. 5 resembles a narrow beam spread, spot-light type illumination with transmitter side field-of-view for long link lengths estimated as 1.7º. As discussed previously, this is a direct consequence of the objective of maximizing the collection efficiency at longer link lengths, close to 300 cm considered here. The VLC transmitter demonstrated here cannot be considered as a generic lighting fixture, as often proposed in previous LED based VLC implementations [1]. The ability to steer beams in indoor setting using spatial light modulators for supporting non-directed line-of-sight communication in the presence of obstructions has been demonstrated recently [28]. Specific use-cases in which the spot-light VLC transmitters developed here can co-exists with generic lighting infrastructure needs to be identified [18]. The observed chromatic effects in the illumination spot and color shifts with propagation distance can be mitigated using customized achromatic lens combinations to simultaneously achieve good communication and illumination performance. This however requires more complex lens design when compared to the simple stock lenses considered here and most of the previous VLC implementations. Another point to highlight is that the optical intensity levels at the receiver plane in the present demonstration are 37 μW/cm^2 and 12 μW/cm^2 for the two optimized link conditions. These intensity levels are approximately three and eight times lower than

the maximum permissible exposure (MPE) limit for ocular exposure for long duration continuous-wave directed blue-green laser of $\sim$100 μW/cm^2 [15], [29]. The low optical intensity levels combined with reduced spatial coherence due to the diffusive phosphor surface can render the above LD-based white light source suitable for eye safe usage in indoor settings.

6. Conclusion

We have demonstrated an optical ray-tracing based approach for minimizing path-loss for indoor laser-based visible light communication system. The optical link design presented here focuses on achieving best communication performance for variable link distances with minimal change to the optical system by finding optimal positions of transmitter and receiver lenses. The path-loss optimization is found to result in narrow beam spread, spot-light type illumination profile directed towards the receiver, to ensure efficient light collection for extended link distances. The illumination source is also experimentally characterized to quantify the beam profile, color rendering and illuminance level as a function of link length. This is found to be in good agreement with the optical ray-tracing simulations. Communication experiments with OOK modulated data at 1.5 Gbps and link distance of 25 cm and 265 cm achieves BER close to 3×10^{-3}. This is achieved for illumination levels of 45 and 16 lx, with optical intensity levels well within the permissible eye-safety limit for the wavelength of interest. A comparison with previous experimental reports shows that the path-loss optimization approach helps achieve gigabit-class communication performance at variable and practically relevant link lengths and at lowest illuminance levels thus far reported. The work presented here emphasizes the importance of optical ray tracing to maximize light throughput in the laser-based white light VLC link and achieve good communication at practically useful link lengths of few meters.

Acknowledgment

The authors also thank Rabindra Biswas, Arpita Mishra, and Vidit Jha for their help with the visible light communication system implementation and characterization.

References

[1] H. Elgala, R. Mesleh, and H. Haas, "Indoor optical wireless communication: Potential and state-of-the-art," *IEEE Comm. Mag.*, vol. 49, no. 9, pp. 56–62, Sep. 2011.
[2] P. H. Pathak, X. Feng, P. Hu, and P. Mohapatra, "Visible light communication, networking, and sensing: A survey, potential and challenges," *IEEE Commun. Surv. Tut.*, vol. 17, no. 4, pp. 2047–2077, Oct./Nov. 2015.
[3] J. Grubor, S. Randel, K. D. Langer, and J. W. Walewski, "Broadband information broadcasting using LED-based interior lighting," *J. Light. Technol.*, vol. 26, no. 24, pp. 3883–3892, 2008.
[4] A. M. Khalid, G. Cossu, R. Corsini, P. Choudhury, and E. Ciaramella, "1-Gb/s transmission over a phosphorescent white LED by using rate-adaptive discrete multitone modulation," *IEEE Photon. J.*, vol. 4, no. 5, Oct. 2012.
[5] G. Cossu, L. Tao, X. Huang, J. Shi, and N. Chi, "8-Gb/s RGBY LED-based WDM VLC system employing high-order CAP modulation and hybrid post equalizer," *IEEE Photon. J.*, vol. 7, no. 6, Dec. 2015, Art. no. 7904507.
[6] S. Rajbhandari *et al.*, "A review of gallium nitride LEDs for multi-gigabitper-second visible light data communications," *Semicond. Sci. Technol.*, vol. 32, no. 2, pp. 1–44, 2017.
[7] D. Tsonev *et al.*, "A 3-Gb/s single-LED OFDM-based wireless VLC link using a gallium nitride μ LED," *IEEE Photon. Technol. Lett.*, vol. 26, no. 7, pp. 637–640, Apr. 2014.
[8] S. Rajbhandari *et al.*, "A multigigabit per second integrated multiple-input multiple-output VLC demonstrator," *J. Lightw. Technol.*, vol. 35, no. 20, pp. 4358–4365, 2017.
[9] C. Lee *et al.*, "2 Gbit/s data transmission from an unfiltered laser-based phosphor-converted white lighting communication system," *Opt. Express*, vol. 23, no. 23, 2015, Art. no. 29779.
[10] H. Chun, S. Rajbhandari, D. Tsonev, G. Faulkner, H. Haas, and D. O'Brien, "Visible light communication using laser diode based remote phosphor technique," in *Proc. IEEE Int. Conf. Commun. Work*, Dec. 2015, pp. 1392–1397.
[11] C. Lee *et al.*, "Gigabit-per-second white light-based visible light communication using near-ultraviolet laser diode and red-, green-, and blue-emitting phosphors," *Opt. Express*, vol. 25, no. 15, 2017, Art. no. 17480.
[12] D. Tsonev, S. Videv, and H. Haas, "Towards a 100 Gb/s visible light wireless access network," *Opt. Express*, vol. 23, no. 2, 2015, Art. no. 1627.
[13] B. Janjua *et al.*, "Going beyond 4 Gbps data rate by employing RGB laser diodes for visible light communication," *Opt. Express*, vol. 23, no. 14, 2015, Art. no. 18746.
[14] P. Battacharya, *Semiconductor Optoelectronic Devices*, 2nd ed. London, U.K.: Pearson Education, 2017.

[15] C. Basu, M. Meinhardt-Wollweber, and B. Roth, "Lighting with laser diodes," *Adv. Opt. Technol.*, vol. 2, no. 4, pp. 313–321, 2013.
[16] American National Standard for Safe Use of Lasers, *ANSI Z136.1* – 2014. Revision of ANSI Z136.1-2007. Laser Institute of America, 2014.
[17] G. Cossu, W. Ali, R. Corsini, and E. Ciaramella, "Gigabit-class optical wireless communication system at indoor distances (15 – 4 m)," *Opt. Express*, vol. 23, no. 12, 2015, Art. no. 15700.
[18] B. Fahs, A. J. Chowdhury, and M. M. Hella, "A 12-m 2.5-Gb/s lighting compatible integrated receiver for OOK visible light communication links," *J. Light. Technol.*, vol. 34, no. 16, pp. 3768–3775, 2016.
[19] "Intematix Corporation, " 2014. [Online]. Available: http://www.intematix.com/technology/chromalit-technology
[20] Z. Ghassemlooy, W. Popoola and S. Rajbhandari, *Optical Wireless Communication: System and Channel Modelling With MATLAB*. Boca Raton, FL, USA: CRC Press, Taylor & Francis, 2013.
[21] J.-Y. Sung, C.-W. Chow, and C.-H. Yeh, "Is blue optical filter necessary in high speed phosphor-based white light LED visible light communications?" *Opt. Express*, vol. 22, no. 17, 2014, Art. no. 20646.
[22] Z. Opticstudio, [Online]. Available: https://www.zemax.com/products/opticstudio
[23] P. M. Butala, H. Elgala, and T. D. C. Little, "SVD-VLC: A novel capacity maximizing VLC MIMO system architecture under illumination constraints," in *Proc. IEEE Globecom Workshops*, 2013, pp. 1087–1092.
[24] T. Chen, L. Liu, B. Tu, Z. Zheng, and W. Hu, "High-spatial-diversity imaging receiver using fisheye lens for indoor MIMO VLCs," *IEEE Photon. Lett.*, vol. 26, no. 22, pp. 2260–2263, Nov. 2014.
[25] C. Lee *et al.*, "Gigabit-per-second white light-based visible light communication using near-ultraviolet laser diode and red-, green-, and blue-emitting phosphors," *Opt. Express*, vol. 25, no. 15, 2017, Art. no. 17480.
[26] C. H. Yeh, C. W. Chow, and L. Y. Wei, "1250 Mbit/s OOK wireless white-light VLC transmission based on phosphor laser diode," *IEEE Photon. J.*, vol. 11, no. 3, Jun. 2019, Art. no. 7903205.
[27] C. Lee *et al.*, "4 Gbps direct modulation of 450 nm GaN laser for high-speed visible light communication," *Opt. Express*, vol. 23, pp. 16232–16237, 2015.
[28] Z. Cao, X. Zhang, G. Osnabrugge, J. Li, I. M. Vellekoop, and A. M. J. Koonen, "Reconfigurable beam system for non-line-of-sight free-space optical communication," *Light Sci. Appl.*, vol. 8, 2019, Art. no. 69.
[29] A. K. Maini, *Lasers and Optoelectronics*. Hoboken, NJ, USA: Wiley, 2013, pp. 599–603.